SHAKE TABLE TESTS OF SEGMENTAL BRIDGE COLUMN WITH MATCH-CAST DRY JOINTS

Wang Zhi qiang[1], Ge Ji ping[2] and Wei Hong yi[3]

[1] *Associate Professor, Dept. of Bridge Engineering , Tongji University, Shanghai, China*
[2] *PHD Student, Dept. of Bridge Engineering , Tongji University, Shanghai, China*
[3] *Professor, Dept. of Bridge Engineering , Tongji University, Shanghai, China*
Email: bridgejiping@126.com

ABSTRACT :

In the paper, the seismic performance of segmental bridge column with match-cast dry joints was investigated through a series of earthquake simulator tests. The research objectives were to investigate the effect of cast-in-placement construction method to pre-cast segmental construction, to compare the damaging effects of existing of energy-dissipating device, and to assess the different dynamic response with the same skeleton curve between cast-in-placement specimen and pre-cast segmental specimen. Then performance of each column was examined using some measures. Comparing the response of each specimen to the same runs, the relative displacement demand of the pre-cast segmental bridge column with samller enengy-dissipation capacity is large than that of a conventional cast-in-place reinforced concrete bridge column.

KEYWORDS: unbonded and bonded strands; dry joints; segmental bridge columns; shake table test

1. RESEARCH BACKGROUND

The research presented here is part of the study to investigate the seismic performance of pre-cast segmental bridge columns. The major focus in the research was on the shake table testing of segmental bridge column with match-cast dry joints. An extensive amount of experimental research has been conducted on the seismic response and performance of segmental bridge under cyclic loading. The column that was subjected to quasi-static loading failed due to low-cycle fatigue of the longitudinal reinforcement. The column that was tested dynamically failed due to rupture of the lateral tie reinforcement. It was concluded that shake table testing of structural elements could lead to results that are different than those obtained from commonly applied slow cyclic loading due to effect of high strain rate combined with variations in loading history (N.S. Johson and M.S. Saiidi, 2006). Shake table testing is the most realistic of the test methods because it includes the most dynamic effects. No available literature discussed the performance of segmental bridge columns on shake table.

This paper presents the results of a series of earthquake simulator tests carried out to investigate the segmental bridge columns. The effects of construction type, the existing of additional energy-dissipating device, and the bond condition were explored experimentally.

2. SPECIMEN DESIGN

Shake table tests were designed to observe the process of dynamic response in segmental bridge columns. The test specimens were composed of four columns fixed at their base separately (Figure 1). Those were a conventional reinforced concrete bridge column (RC), a precast segmental unbonded prestressing reinforced concrete bridge column (UBPC-S), a precast segmental unbonded prestressing reinforced concrete bridge column with energy-dissipating rebars (UBPC-SD), a precast segmental bonded prestressing reinforced concrete bridge column (BPC-S). Specimen UBPC-S, UBPC-SD and BPC-S mainly consist of one solid block for loading, five precast rectangular solid segments, and one solid block for foundation. For specimen UBPC-SD, Grade I D10 is the longitudinal mild steel reinforcement being extended across the segment joints and is

referred as energy dissipation bars in the paper. No shear keys exist in the adjacent segments. All these test specimens are independent columns standing on a footing, and having a solid rectangular area of 180 mm x 240 mm in the cross section. The height from the bottom of the column to the center of gravity of the top mass is 1.8 m, resulting in an effective aspect ratio of 7.5. The concrete is designed to be C40. The same reinforcement is used for all specimens. The columns are reinforced with 10 No. 10 (10mm-diameter) deformed bars and No. 6 (6 mm-diameter) stirrups at 80 mm pitch. The longitudinal reinforcement ratio and the volumetric ratio of stirrups reinforcement are 1.82% and 1.1%, respectively. The reinforcing bars with expected yield strength of 335 MPa (HRB335) are used for both longitudinal and hoop reinforcement. The prestressing tendons in UBPC-S, UBPC-SD and BPC-S consist of two 12.7 mm (7D4 mm) diameter low-relaxation steel prestressing strands with expected ultimate strength of 1860 MPa. A scaling factor of 5 is assumed for the specimens. All specimens supported a mass of 116 kN, producing column axial load stresses roughly equivalent to those expected for actual bridge column and the resulting dead load ratio is 10%. A prestressing force of 130 kN is applied to the column UBPC-S, UBPC-SD and BPC-S, resulting in a axial force ratio of 11.2% and the axial stress in the concrete of 3MPa. The applied dead load to the all column was 116 kN. So the total axial force ratio of column UBPC-S, UBPC-SD and BPC-S is 21.2%.

The test specimens were constructed in an upright position in a casting site adjacent to the earthquake simulator. Reinforcement cages were assembled and instrumented with strain gauges. Normal-weight aggregate concrete was cast in one lifts. Companion prismatic block cured for 28 days were stored with the specimens and the average strength of concrete was measured as 43.2 MPa. Table 1 shows the mechanical properties of steel materials.

Table 1 Mechanical properties of steel reinforcement and PC strands

| Type	Rebar			PC strands
	d=6mm	Grade II d=10mm	Grade I d=10mm	7D5 mm
Yield strength（MPa）	470	350	340	N/A
Tensile strength（MPa）	540	490	500	1500
Extending ratio（%）	25	35	33	N/A

Each test specimen was moved to the earthquake simulator prior to testing. A concrete box full of steel weights was placed on the top of specimen to simulate gravity loads and inertial mass. The weights were then bolted in position so they moved in unison with the test specimen.

Instrumentation consisted of displacement transducers to measure horizontal displacements of the mass and local deformations of the plastic hinge region, accelerometers to measure horizontal accelerations of the mass, strain gages on selected reinforcing bars and prestressing strands.

3. GROUND MOTIONS AND TEST SEQUENCE

All specimens were subjected to one horizontal component from scaled El Centro (NS component, 1940) earthquake ground record. For simplicity, no vertical accelerations were considered. The record was scaled assuming a length scale factor of 5 which is consistent with the scale of the specimen, hence, the time duration of the record was reduced by 2.24($\sqrt{5}$) while the acceleration was kept the same, and then scaled the magnitude of acceleration to the desired testing level.

Each of the tests started with a series of white noise tests to estimate the natural period and the damping ratio of each specimen. To investigate the seismic capacity and dynamic response of the testing model, the earthquake waves were scaled to the peak ground acceleration (PGA) of 0.1g to 0.8g with incremental value of 0.1g. For specimen RC, UBPC-S, UBPC-SD and BPC-S, the ending PGA was 0.8g, 0.6g, 0.6g, 0.7g respectively. After the completion of each input stage, the damage process and crack distribution of the model were observed and recorded.
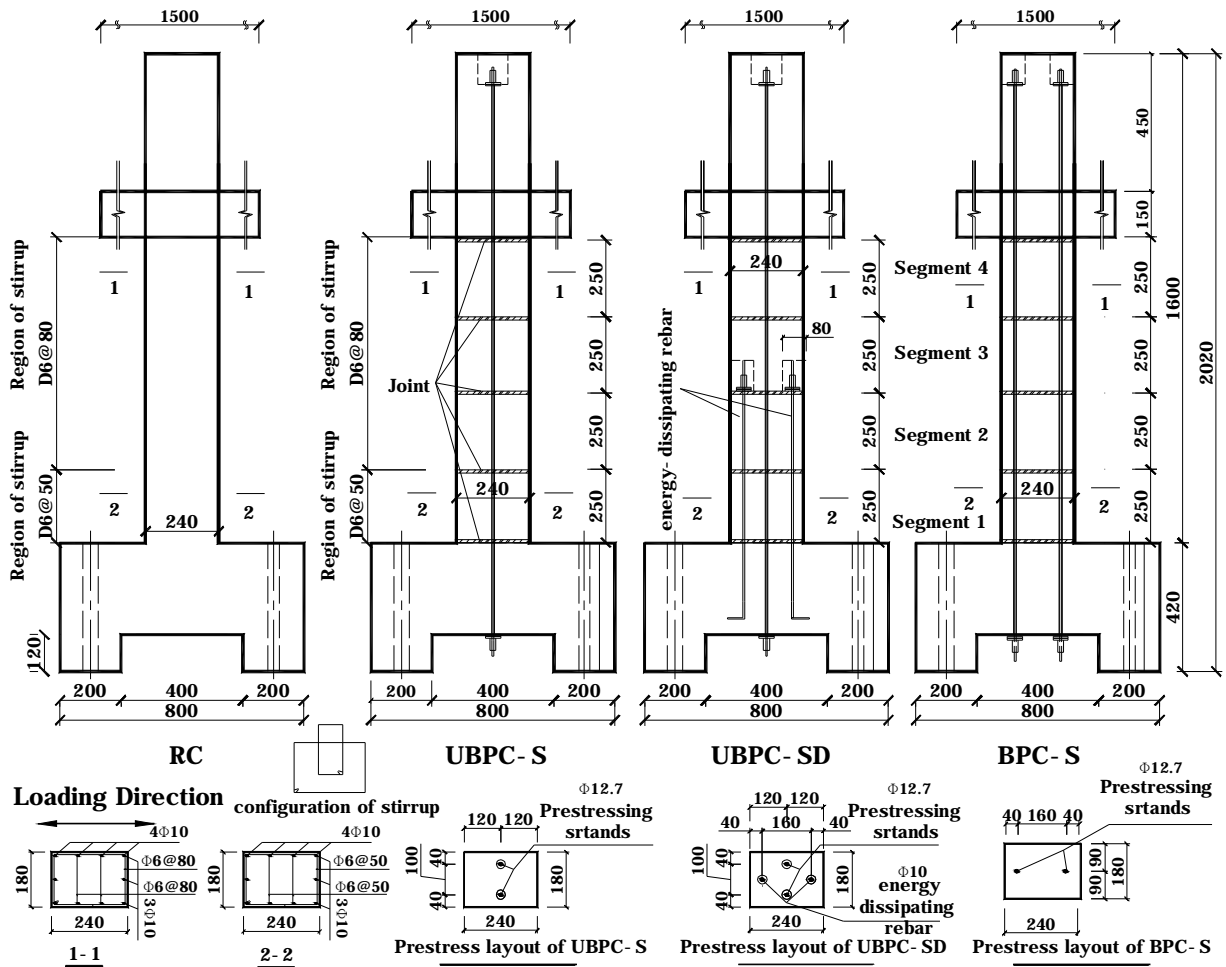
(a) Detail of section and main features of specimens
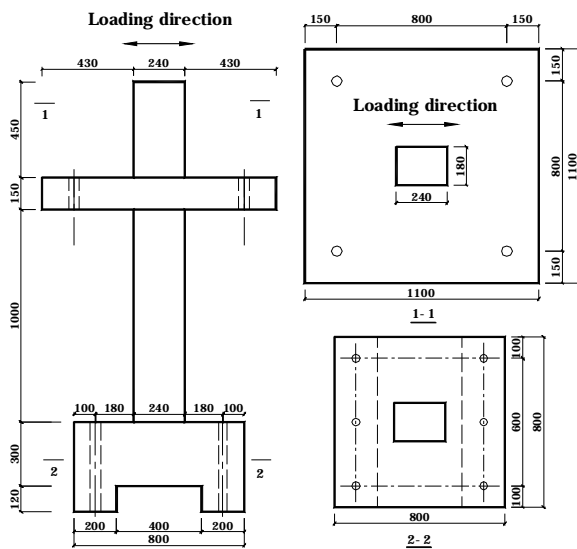
(b) Detail of configuration   (c) Photo of test specimen on shaking table
Figure 1 Shake table test specimen (units in mm)

4. TEST RESULTS AND DISCUSSION

4.1 Achieved shake table motions

Before studying the effect of the ground motion excitations on the specimens, it is desirable to investigate the performance of the shaking table. Performance is defined as the ability of the shaking table to accurately reproduce the input signal. Figure 2 compared the processed records used (input) to the actual shaking table recorded motion (output) corresponding to the 0.1g PGA motion run for specimen UBPC-S, includes plots of the Fourier spectrum and of the elastic response spectra. It is shown that the input signals are reproduced with a fair degree of accuracy for the selected run. And the remaining part of the excitation also matches well with the other runs.
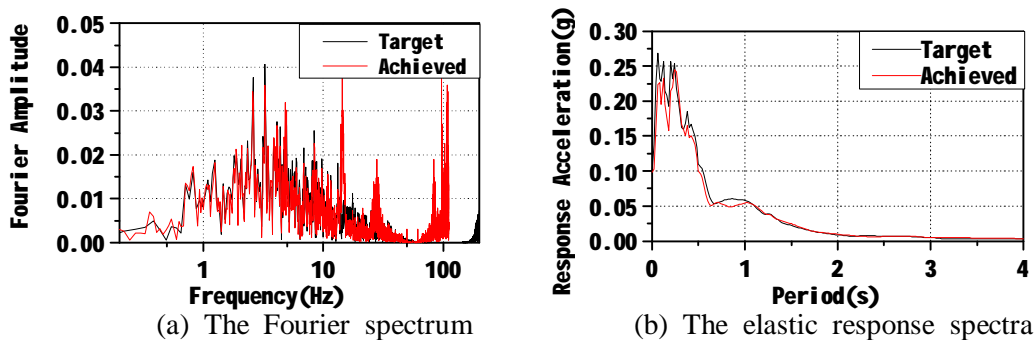
      (a) The Fourier spectrum   (b) The elastic response spectra

Figure 2 Shaking table input and recorded time history of 0.1g PGA motion

4.2 Observed Results

This section describes the physical behavior of the four specimens. Video recording was used to document the damage progression in the plastic hinge region during each dynamic test. Overall, initial flexural cracking in the columns began corresponding to the 0.2g PGA motion, and then the following development of crack is different for each specimen. No permanent damage was observed in any of the specimen to the maximum level earthquake, only minor cracking was observed up to that level, and most cracks closed completely by the end of test.

Photographs of maximum damage state are shown in Figure 3. For specimen RC, cracking was more concentrated at the bottom of the column near the footing as would expect. No spalling was observed near the base of the column. The measured permanent deformation was generally small. This shows that the column would exihibit an excellent performance during a function-evaluation level earthquake. Since no spalling and bar buckling occurred at the base during the maximum level event, the specimen could sustain a larger level earthquake without collapsing. For the three precast segmental specimen, no cracks were observed in the body of segmental column. In the maximum earthquake excitation, a large crack formed at the interface with the footing (Figure 3(b) and 3(d)).s. The cracks also closed completely by the end of test. So the crack was larger and concentrated at the base segment joint for the segmental columns, while the crack was thin and more for specimen RC.

      (a) RC（0.8g PGA motion）   (b) UBPC-S（0.6g PGA motion）

(c) UBPC-SD (0.6g PGA motion)   (d) BPC-S（0.7g PGA motion）

Figure 3 Photos of maximum crack state in the maximum excitation of each specimen

4.3 Modal frequencies

The white noise runs could be used to calculate the period of vibration and the mode shape. The idealized mode shape and the tested mode shape are shown in Figure 4. White noise test was commonly included in test schedule to allow for calculation of the change in frequency response of the bridge as a measure of damage progression. Instead, the the stochastic subspace identification method (D.J. Yu and W.X. Ren, 2005) is used to identify the frequency of vibration. The plots of frequency for the first and second mode vs. input earthquake excitation levels are shown in Figure 5. From the estimated frequency value, the effective stiffness of the column can be calculated. The relationship of frequency decrease to the PGA of excitation is expected because the damage increasing with PGA of excitation.
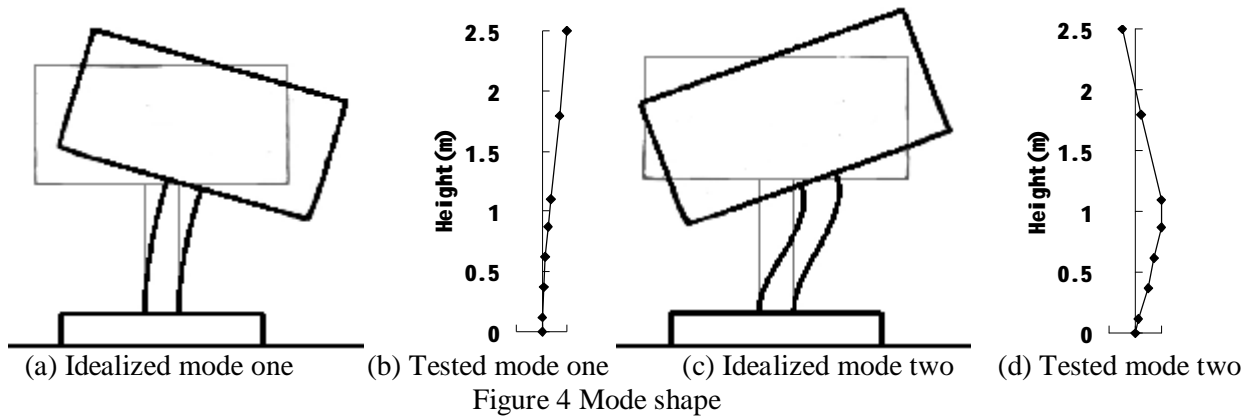
(a) Idealized mode one   (b) Tested mode one   (c) Idealized mode two   (d) Tested mode two
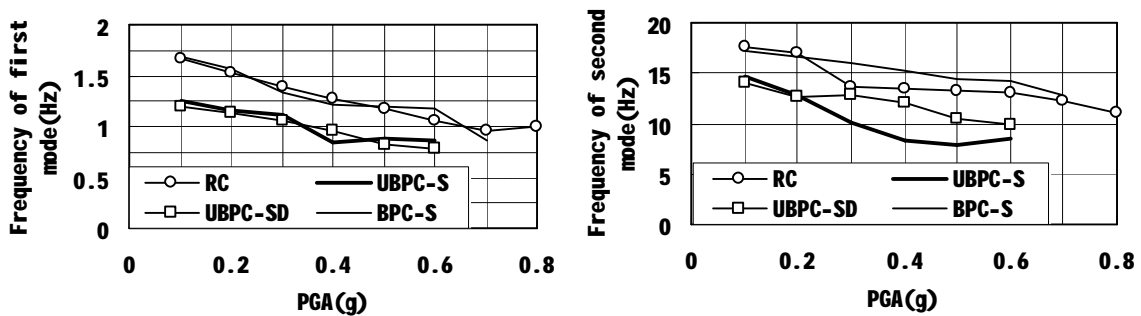
Figure 4 Mode shape

Figure 5 Frequency from stochastic subspace identification method vs. input earthquake excitation levels

4.4 Displacement response

The complete relative displacement histories of each specimen are plotted in Figure 6. Those plots' provide a

global view of all shaking runs performed on each specimen, including the offset of the displacement baseline because of residual displacement. Figure 7 gives the maximum relative displacement of each specimen vs. input earthquake excitation levels. It is shown that the relative displacement demand of segmental bridge column is larger than that of specimen RC. Before the 0.7g PGA motion, the relative displacement demand for specimen BPC-S is very close to specimen RC. But the relative displacement demand for specimen BPC-S increases suddenly from 0.6g PGA motion to 0.7g PGA motion.
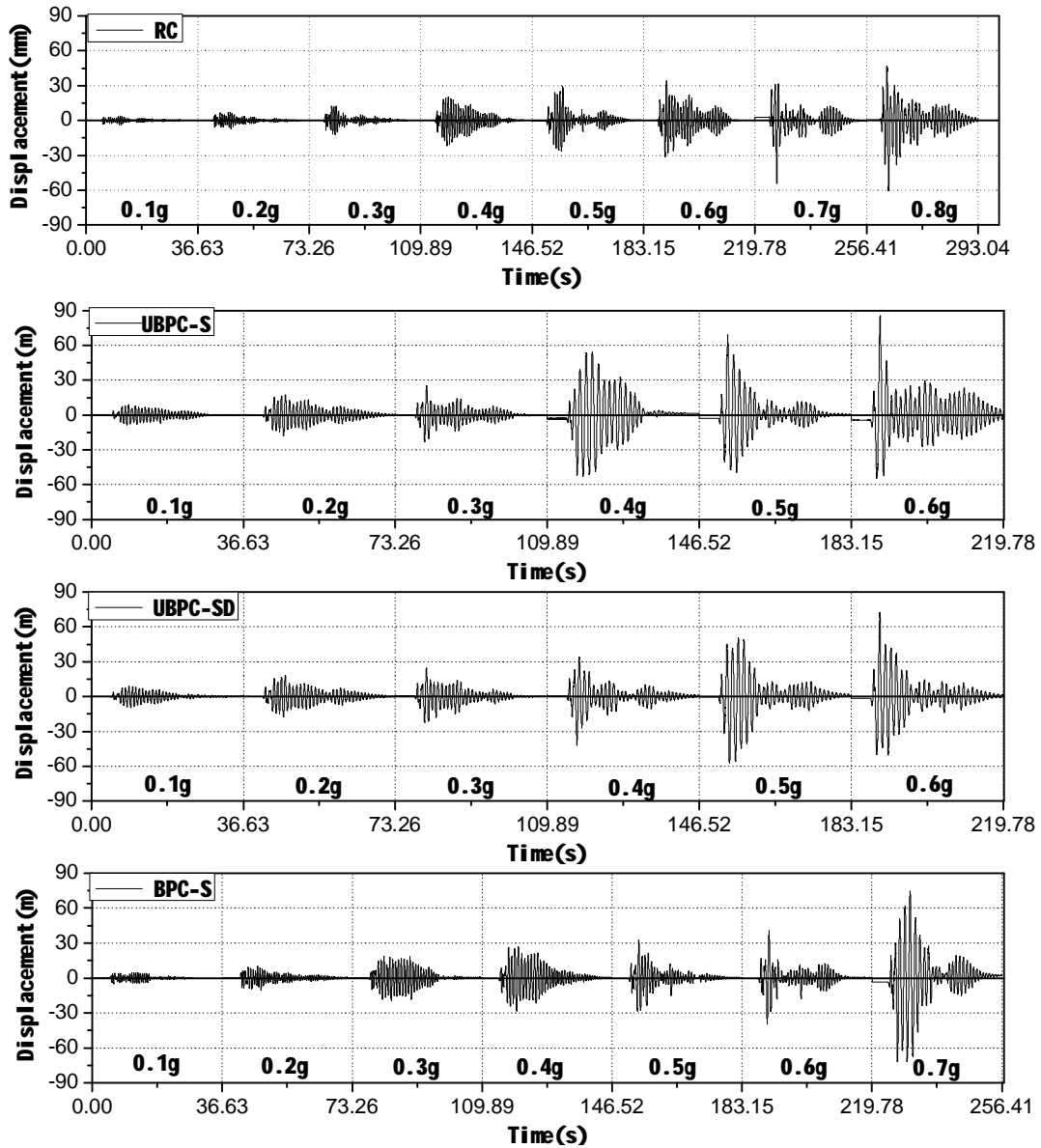
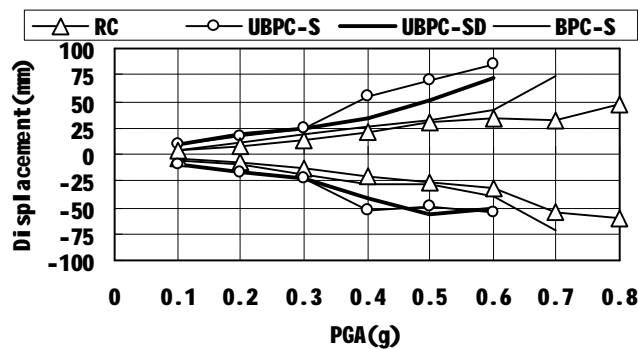Figure 6 Complete relative displacement histories of each specimen

Figure 7 Maximum relative displacement of each specimen vs. input earthquake excitation levels

4.5 Force-displacement hysteresis

To draw force-displacement hystereses, the lateral force at the center of mass is obtained by the product of acceleration and the mass of that using Newton's second law. It can be seen in the Figures 8 that all specimen underwent large deformation and dissipated considerable amount of hysteretic energy. A goal of the specimen BPC-S design is that the column size, stiffness, and strength similar to standard RC column (Figure 9), so that the reductions in residual displacement and the increase in peak displacement demand could be directly compared between the two system. Specimen BPC-S with smaller energy-dissipation capacity performs poorly, the column's response is larger than that of a conventionally designed reinforced concrete column RC.
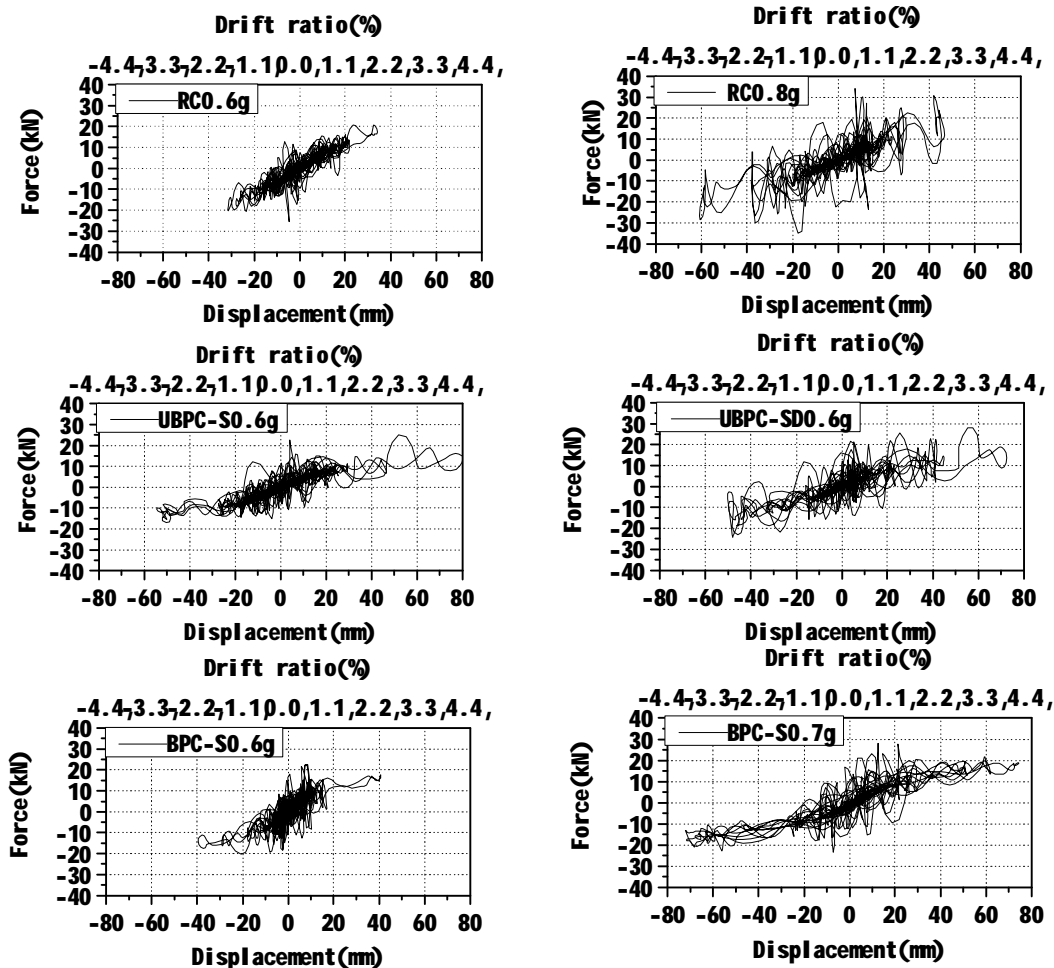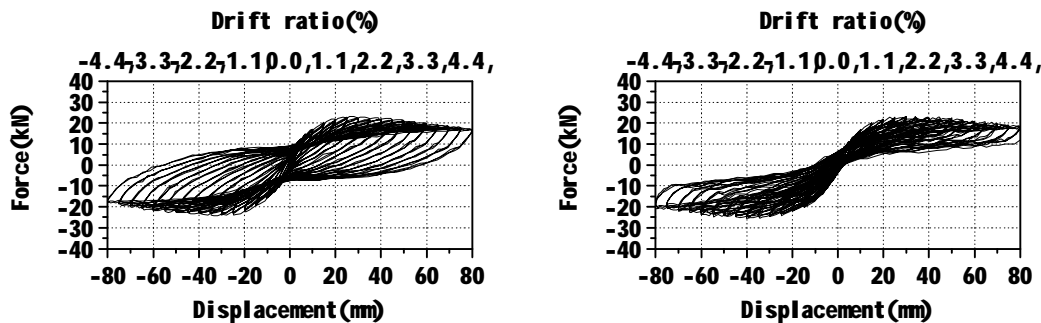
Figure 8 Force-displacement hystereses at critical earthquake excitation level

(a) RC   (b) BPC-S

Figure 9 Force-displacement hystereses from cyclic loading test

5. CONCLUSION

The paper discusses the observed behavior and the measured results from the shake table testing of segmental bridge column. The purpose was to improve the understanding of segmental bridge column. The main conclusions drawing from the research are presented in the following.

1. The four specimen exhibited stable ductile behavior under the selected excitation. Damage visible after these test consisted of minor spalling of the unconfined cover at the column base and evidence of cracks that had formed had formed during the excitations but had subsequently closed. The crack was larger and concentrated at the base segment joint for the segmental columns, while the crack was thin and more for specimen RC. Those specimens were still able to resist greater level earthquake.

2. Comparing the response of each specimen to the same runs, the pre-cast segmental bridge column with samller enengy-dissipation capacity performs poorly. The response of the column is large than that of a conventional cast-in-place reinforced concrete bridge column.

ACKNOWLEDGEMENTS

REFERENCES

Stephen A. Mahin and Junichi Sakai. (2006). Use of Partially Prestressed Reinforced Concrete Columns to Reduce Post-Earthquake Residual Displacements of Bridges. Fifth National Seismic Conference on Bridges & Highways, San Francisco, CA, September 18-20, Paper No. B25.

Mahmoud M. Hachem, Stephen A. Mahin and Jack P. Moehle. (2003). Performance of circular reinforced concrete bridge columns under Bidirectional earthquake loading. Report No. PEER 2003/06, Berkeley: Pacific earthquake engineering research center, University of California.

Nathan S. Johnson, M. "Saiid" Saiidi, David H. Sanders. (2006). Large-scale experimental and analytical seismic studies of two-span reinforced concrete bridge system. Report No. CCEER-06-02, Center for Civil Engineering Earthquake Research, Department of Civil and Environmental Engineering, University of Nevada, Reno, Nevada.

Dan-Jiang Yu and Wei-Xin Ren. (2005). EMD-based stochastic subspace identification of structures from operational vibration measurements. *Engineering Structures* **27:12**, 1741-1751.